

SELECTED ADVANCES IN THE ACCELERATOR DESIGN OF THE FUTURE CIRCULAR ELECTRON-POSITRON COLLIDER (FCC-ee)*

A. Chance, B. Dalena, CEA, Paris, France; K. Andre, H. Bartosik, J. Bauche, X. Buffat, J. Keintzel, R. Kersevan, L. Mether, R. Tomas, A. Vanel, L. Von Freeden, F. Zimmermann[†], CERN, Meyrin, Switzerland; I. Agapov, E. Musa, A. Rajabi, R. Wanzenberg, DESY, Hamburg, Germany; P. Kicsiny, T. Pieloni, L. Sabato, L. van Riesen-Haupt, Y. Wu, EPFL, Lausanne, Switzerland; S. Liuzzo, S. White, ESRF, Grenoble, France; E. Gianfelice, P. Raimondi, FNAL, Batavia, U.S.A.; A. Ghribi, GANIL, Caen, France; M. Migliorati, Sapienza, Rome, Italy; I. Chaikovska, IJCLab, Paris, France; C. Milardi, M. Zobov, INFN, Italy; K. Ohmi, KEK, Tsukuba, Japan; P. Craievich, M. Koratzinos, R. Zennaro, PSI, Villigen, Switzerland; X. Huang, T.O. Raubenheimer, SLAC, Stanford, U.S.A.; F. Yaman[‡], STFC, Warrington, U.K.; K.B. Cantun, UADY, Merida, Mexico; K. Oide[§], UNIGE, Geneva, Switzerland; H. Maury, UGTO, Guanajuato, Mexico; on behalf of the FCC Collaboration

Abstract

In autumn 2023, the FCC Feasibility Study underwent a crucial “mid-term review”. We describe some accelerator performance risks for the proposed future circular electron-positron collider, FCC-ee, identified for, and during, the mid-term review. For the collider rings, these are the collective effects when running on the Z resonance – especially resistive wall, beam-beam, and electron cloud –, the beam lifetime, dynamic aperture, alignment tolerances, and beam-based alignment. For the booster, the primary concern is the vacuum system, with regard to impedance and effects of the residual gas. For the injector, the layout and the linac repetition rate are primary considerations. We discuss the various issues and report the planned mitigations.

FCC-FS MID-TERM REVIEW

In 2021, the FCC Feasibility Study (FCC-FS) was launched [1, 2] in response to a recommendation from the 2020 update of the European Strategy for Particle Physics [3]. After three years of work, the mid-term review report [4] was published, covering the placement of the ring and the implementation of the facility, civil engineering, technical infrastructure, accelerators, physics opportunities and detector concepts, and cost and funding aspects. A mid-term review [5] took place in three steps, starting in October 2023 with dedicated reviews by two expert committees and by the CERN Council’s subordinate bodies, the Scientific Policy Committee and the Finance Committee, and culminating in an extraordinary session of the CERN Council in February 2024. Before and during this mid-term review, several performance risks were highlighted, motivating various design choices or changes. In this paper, we discuss some of these, which are of particular importance for the FCC-ee accelerator design.

* Work supported by the European Union’s H2020 Framework Programme (grant no. 951754, FCCIS) and by the Swiss CHART programme.

[†] frank.zimmermann@cern.ch

[‡] also at IYTE, Izmir, Türkiye

[§] also at KEK, Tsukuba, Japan

IMPEDANCE-DRIVEN INSTABILITIES

In the collider rings, the impedance-related effects are most severe for the Z mode, since here the beam energy is the lowest (45.6 GeV), and the beam current the highest (1.3 A). Combined with the large circumference (91 km) this leads to a fast transverse coupled-bunch instability at low frequency, driven by the resistive wall of the arc vacuum chamber, with a rise time of 1.4 ms, or about 4 turns, at a frequency around 2.6 kHz. For this unstable mode all bunches oscillate in phase. A narrow-band feedback could specifically act on this fastest growing coupled-bunch mode, in addition to a slower bunch-by-bunch feedback system [6]. Concerning single-bunch effects, the “-1 mode” transverse instability is induced by an interplay of the impedance with the feedback. The predicted intensity threshold is above the nominal beam current. However, did it unexpectedly occur, this instability could be suppressed by increasing the chromaticity or by adjusting the bunch-by-bunch feedback system.

BEAM-BEAM AND LIFETIME

Particle-in-cell (PIC) simulations of the beam-beam collisions and tracking using a soft-Gaussian approximation are both available in various codes (Xsuite, BBSS, sctr, Life-trac), together with either a linear or the full nonlinear optical lattice. The most challenging case to model is the Z pole operation. Using a GPU based code (sctr), tracking of the beam-beam collision and the simulation of the nonlinear optics require comparable CPU time. In simulations with the full nonlinear lattice, the design luminosity is achieved for both Higgs and Z modes, as is illustrated in Fig. 1. No large difference is observed between the PIC results and the soft Gaussian approximation. In parallel, the interplay of beam-beam collisions with the longitudinal impedance has also been studied [7]. Using a weak-strong beam-beam simulation, taking into account the dynamic aperture, synchrotron radiation and beamstrahlung, the equilibrium emittance and beam lifetimes are computed by SAD. A result for the $\bar{t}\bar{t}$ mode of operation is shown in Fig. 2.

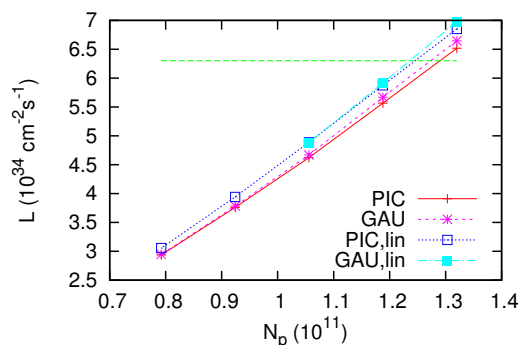


Figure 1: Luminosity for the FCC-ee Higgs mode, as a function of bunch population, simulated with PIC code or soft Gaussian approximation (“GAU”), and considering either the full nonlinear lattice or only the linear optics (“LIN”). The design bunch population is $N_b = 1.32 \times 10^{11}$, and the target luminosity $L = 6.3 \times 10^{34} \text{ cm}^2 \text{ s}^{-1}$ (the green line).

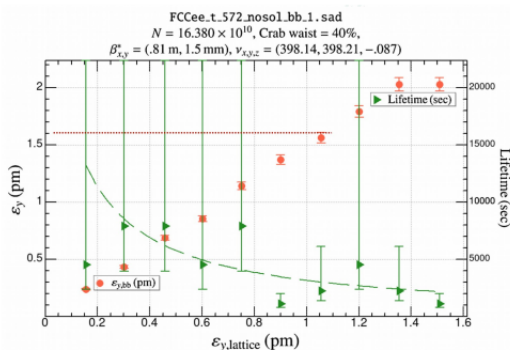


Figure 2: Beam lifetime (green) and equilibrium vertical emittance (red) as function of the vertical emittance without collisions, as simulated by SAD.

ELECTRON CLOUD

Electron cloud formation is a concern for the FCC-ee Z mode. We report a few key findings from the mid-term report. To avoid the electron-cloud induced single-bunch instability [8], the average central electron cloud density prior to bunch arrival should be lower than about $\rho_{\text{thr}} \approx 2 \times 10^{10} \text{ m}^{-3}$ [9–11]. To stay below this threshold, both secondary emission and primary photoemission need to be controlled and minimized. The secondary emission yield of the surface wall is kept low by a novel NEG coating with a thickness of $\sim 150 \text{ nm}$ [12]. The number of photoelectrons emitted inside the central chamber is confined by the aperture slits with antechamber and photon absorbers located around the horizontal plane.

Electron cloud build-up simulations show a strong dependence on the bunch spacing as well as on the bunch intensity [11]. To identify a viable operational scenario, four different filling schemes with different bunch spacing, train length and bunch population, corresponding to equal total current, were examined as summarised in Table 1, where Case 3 is similar to the present baseline. A bunch spacing of at least 20 ns is required to avoid severe electron-cloud

Table 1: Four Alternative Beam Patterns with Different Bunch Population N_b and Spacing t_{sep} Considered for Electron-Cloud Simulations

Name	N_b [10^{10}]	t_{sep} [ns]	bunches/train
Case 1	15	15	320
Case 2	21.5	20	280
Case 3	21.5	25	560
Case 4	24.3	25	255

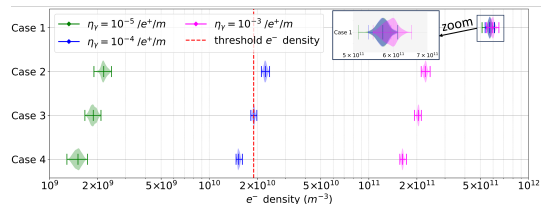


Figure 3: Simulated central electron density for a maximum secondary emission yield $\delta_{\text{max}}=1.2$ [15], and three primary photoelectron rates considering the four cases of Table 1 [4, 11]. Red line indicates the approximate threshold.

effects. For the mid-term review, parameters with a bunch spacing of 25 ns were adopted, which is the same as for LHC. Simulation results for different photoelectron rates displayed in Fig. 3 suggest that a primary photoelectron rate of the order of $10^{-4}/e^+/m$ is the maximum that can be tolerated.

In an FCC-ee dipole, a passing 45.6 GeV positron emits $dN/ds \approx 5\alpha\gamma/(2\sqrt{3}\rho) \approx 0.1$ synchrotron-radiation photons per metre, where $\rho \approx 9.9 \text{ km}$ is the bending radius. If, slightly optimistically, it is assumed that the photoelectron yield η_e of the NEG coated chamber is 0.1 (Ref. [13] reported $\eta_e \approx 0.25$), in order to reach a primary photoelectron rate as low as $10^{-4}/e^+/m$, the antechamber with its photon stops must absorb 99% of the photons without reflection into the circular part of the vacuum chamber. That is, the FCC-ee antechamber should reduce the relevant primary photoelectron rate by about a factor of 100. For comparison, beam measurements at KEK showed that differently shaped antechambers yielded a reduction by only a factor of 4 [13] or 5 [14]. In the future, we will further explore this point.

ALIGNMENT TOLERANCES & BBA

Two optics were developed, named the Global Hybrid Correction (GHC) and Local Chromatic Correction (LCC) optics, respectively. Table 2 presents the rms misalignments of arc quadrupoles and sextupoles leading to 1% rms beta beating or 1 mm rms spurious vertical dispersion, for the Z mode. The results show that LCC holds the promise of more relaxed tolerances for the arc. For the interaction region the differences are less pronounced and sensitivities tighter [16]. Work on the LCC dynamic aperture is still in progress, especially for the higher beam energies.

The initial mechanical pre-alignment shall be improved by beam-based alignment (BBA). For a machine as large as the FCC-ee, parallel BBA (PBBA) is desired, where the centers of multiple quadrupoles or sextupoles are determined

Table 2: Magnet Misalignments Leading to 1% rms Beta Beating or 1 mm rms Dispersion

Optics	$\Delta\beta_x/\beta_x$	$\Delta\beta_y/\beta_y$	D_y
GHC quadr.	2.9 μm	0.7 μm	0.1 μm
LCC quadr.	6.1 μm	0.5 μm	0.26 μm
GHC sext.	17 μm	8.5 μm	2.6 μm
LCC sext.	>100 μm	46 μm	10 μm

Table 3: Booster Parameters at Injection (20 GeV).

parameter	symbol	value	unit
bunch population	N_b	2.4	10^{10}
bunch spacing	t_{sep}	25	ns
no. bunches/train	n_b	255	—
hor. (vert.) emittance	$\varepsilon_{x(y)}$	0.26	nm
av. hor. (vert.) β function	$\langle\beta_{x(y)}\rangle$	~ 50	m
av. hor. (vert.) beam size	$\langle\sigma_{x(y)}\rangle$	~ 100	μm
transv. ampl. damping time	τ_x	~ 3	s
IBS emittance growth rate	$d\varepsilon_x/dt$	~ 0.02	nm/s

at the same time. Two PBBA methods for quadrupoles were explored in simulations [17, 18]. Considering 1 μm BPM noise, residual systematic errors of the PBBA are of order 10–30 μm [18]. One source of systematic error is the orbit angle at the rather long quadrupoles.

BOOSTER VACUUM

FCC-ee features a full-energy booster synchrotron in the collider tunnel. The booster vacuum system is conceived without NEG coating and without bake-out. The outer arc vacuum chamber radius should not exceed 32.5 mm, to avoid a significant increase in the weight and cost of the magnets. At this chamber size, for impedance reasons, a copper vacuum chamber is preferred, and a 1–1.5 mm thick Cu chamber appears to still be acceptable with regard to field errors due to eddy current during the ramp. Changing the chamber of the booster from copper to stainless steel would greatly increase the longitudinal and transverse impedance. Baseline parameters for the booster are compiled in Table 3.

A representative residual gas component in accelerator vacuum systems is CO with an ionization cross section of $\sigma_{\text{ion}} \approx 2$ Mbarn [19], corresponding to an ion generation rate of $\lambda'_{\text{ion}} \approx 6 \text{ m}^{-1}$ per electron at 1 nTorr and 300 K.

In a Gaussian approximation [20] the emittance growth due to multiple gas scattering is

$$\left\langle \frac{d\varepsilon_{x,y}}{dt} \right\rangle \approx \frac{1}{2} \langle \beta_{x,y} \rangle \left(\frac{14.1 \text{ MeV}/c}{p} \right)^2 \frac{m_{\text{CO}} p_{\text{CO}} c}{k_b T X_{0,\text{CO}}}. \quad (1)$$

Considering $m_{\text{CO}} = 14 \text{ g/mol}$, $T = 300 \text{ K}$, $X_{0,\text{CO}} \approx 40 \text{ g cm}^{-2}$ (similar for N_2 and CO_2) we obtain $\langle d\varepsilon_{x,y}/dt \rangle \approx 5 \times 10^{-5} \text{ (m/s)} p_{\text{CO}} [\text{Pa}]$. This growth does not exceed the one due to IBS if $p_{\text{CO}} \leq 4 \times 10^{-7} \text{ Pa}$ or $p_{\text{CO}} \leq 3 \text{ nTorr}$.

Table 4: Alternative Z-mode Booster Cycles for One Beam

bunches/cycle	11,200	1,120
pressure tolerance [nTorr]	~ 1	~ 30
injection time [s]	28	2.8
ramp up & down [s]	0.7	0.7
no. cycles	1	10
full injection [s]	~ 29	~ 35

The ion-induced tune shift along a train of n_b bunches is $\Delta Q_y = r_e \langle \beta_y \rangle C \lambda_{\text{ion}} N_b n_b / (2\pi\gamma\sigma_y(\sigma_x + \sigma_y)) \approx 10^{-8} p [\text{Torr}]$. For $\Delta Q_y < 0.1$ we require $p_{\text{CO}} \leq 1 \text{ nTorr}$.

The jitter amplification by the fast beam-ion instability (FBII) leads to a bunch motion at the end of a train of [21]: $\langle y(i = n_b)^2 \rangle \approx \langle y(0)^2 \rangle \exp(\tau_d / (2\tau_c)) / (4n_b)$, where τ_c is the sub-exponential FBII growth time [22], and τ_d the feedback damping time. Considering only Schottky noise for the first bunch, $\langle y(0)^2 \rangle \approx \sigma_y^2 / N_b$, and a τ_d of 10 turns, at a pressure $p_{\text{CO}} \approx 1.7 \text{ nTorr}$, the oscillation amplitude of the last bunch becomes comparable to the rms beam size.

The ion-related effects are largely mitigated by operating with fewer bunches per cycle. In addition, with fewer bunches the time spent on the injection plateau is reduced, and hence, overall, a larger vacuum pressure could be tolerated. Table 4 compares two scenarios. Operation with fewer bunches has other benefits, such as lower peak RF power and more relaxed machine protection.

OPTIONAL INJECTOR LAYOUT

The current positron yield estimate would allow for producing positrons at a lower electron beam energy of 2.86 GeV, possibly in combination with a Damping Ring (DR) at the same energy. For a schematic layout see Ref. [4]. In this scenario, all linacs operate at a maximum rate of 200 Hz, with 2 bunches per pulse, and no 400 Hz linac operation [4] would be necessary. A dedicated linac up to 2.86 GeV also leads to considerable simplification in operation, and with this layout, no positron return line and arc are required. The same DR as used for the positrons can also accommodate the electrons, stabilizing the downstream beam parameters. The linac repetition rate could be further reduced by accelerating 4 instead of 2 bunches per pulse, if the beam loading with variable bunch charges can be handled.

The DR, complemented by polarisation wigglers, could also be used to pre-polarise pilot bunches (compare [23, 24]), which might avoid the pre-polarisation time otherwise required in the collider at the start of each fresh fill. The polarisation rate with asymmetric wigglers, and the stronger wiggler poles of total length L^+ and bending radius ρ^+ , is approximately [25] $1/\tau_p \approx F\gamma^5 L^+ / \rho^{+3}$, where $F = (5\sqrt{3}/8)r_e \hbar / (m_e c)$. At 2.86 GeV beam energy, with $C \approx 400 \text{ m}$, $\rho^+ \approx 2 \text{ m}$ (4.8 T field), and $L^+ \approx 5 \text{ m}$, the polarisation time in the damping ring, from the wiggler alone, would be about 5 minutes.

REFERENCES

- [1] CERN Council, “Main deliverables and timeline of the FCC feasibility study”, Rep. CERN/SPC/1161; CERN/3588, 2021. <https://cds.cern.ch/record/2774007>
- [2] CERN Council, “Organisational structure of the FCC feasibility study”, Rep. CERN/SPC/1155/Rev.2; CERN/3566/Rev.2, 2021. <https://cds.cern.ch/record/2774006>
- [3] European Strategy Group, “2020 Update of the European Strategy for Particle Physics”, Rep. CERN-ESU-013, 2020. doi:10.17181/ESU2020
- [4] FCC Feasibility Study Midterm Report, 2024, doi:10.17181/mhas5-1f263,
- [5] CERN Management, “FCC Feasibility Study: plans and deliverables for the 2023 mid-term review”, Rep. CERN/SPC/1183/Rev.2; CERN/3654/Rev.2, 2022. <https://cds.cern.ch/record/2838409>
- [6] S. Chen and G. Lopez, “Simulation Studies of the Transverse Dipole Mode Multibunch Instability for the SSC Collider”, Rep. SSCL-614, Jan. 1993. doi:10.2172/10163932
- [7] M. Migliorati, E. Carideo, D. De Arcangelis, *et al.*, “An interplay between beam–beam and beam coupling impedance effects in the Future Circular e e Collider”, *Eur. Phys. J. Plus*, 2021. doi:10.1140/epjp/s13360-021-02185-2
- [8] K. Ohmi and F. Zimmermann, “Head-Tail Instability Caused by Electron Clouds in Positron Storage Rings”, *Phys. Rev. Lett.*, vol. 85, no. 18, pp. 3821–3824, 2000. doi:10.1103/PhysRevLett.85.3821
- [9] Kazuhito Ohmi, “Beam–beam and electron cloud effects in CEPC/FCC-ee”, *International Journal of Modern Physics A*, vol. 31, no. 33, p. 1644014, 2016. doi:10.1142/S0217751X16440140
- [10] K. Ohmi, F. Zimmermann, and E. Perevedentsev, “Wake-field and fast head-tail instability caused by an electron cloud”, *Phys. Rev. E*, vol. 65, no. 1, p. 016502, 2001. doi:10.1103/PhysRevE.65.016502
- [11] F. Yaman, G. Iadarola, R. Kersevan, *et al.*, “Mitigation of electron cloud effects in the FCC-ee collider”, *EPJ Techn Instrum*, vol. 9, no. 9, 2022. doi:10.1140/epjti/s40485-022-00085-y
- [12] E. Belli *et al.*, “Electron cloud buildup and impedance effects on beam dynamics in the Future Circular e⁺e⁻ Collider and experimental characterization of thin TiZrV vacuum chamber coatings”, *Phys. Rev. Accel. Beams*, vol. 21, no. 11, p. 111002, 2018. doi:10.1103/PhysRevAccelBeams.21.111002
- [13] Y. Suetsugu, K. Kanazawa, K. Shibata, and H. Hisamatsu, “Continuing Study on the Photoelectron and Secondary Electron Yield on TiN Coating and NEG (Ti-Zr-V) Coating under Intense Photon Irradiation at the KEKB Positron Ring”, *Nucl. Instrum. Meth. A*, vol. 556, pp. 399–409, 2006. doi:10.1016/j.nima.2005.10.113
- [14] Y. Suetsugu *et al.*, “Mitigating the electron cloud effect in the SuperKEKB positron ring”, *Phys. Rev. Accel. Beams*, vol. 22, no. 2, p. 023201, 2019. doi:10.1103/PhysRevAccelBeams.22.023201
- [15] F. Zimmermann, “Electron-cloud simulations for SPS and LHC”, in *10th Workshop on LEP - SPS Performance: Chamonix X*, Jan. 2000, pp. 136–149.
- [16] S. Liuzzo P. Raimondi S. White, “Updated sensitivities and comparisons of DA and tune working point scans”, presented at the 178th FCC-ee Optics Design Meeting & 49th FCCIS WP2.2 Meeting, 25 January 2024, unpublished. <https://indico.cern.ch/event/1380377/>
- [17] Xiaobiao Huang, “Simultaneous beam-based alignment measurement for multiple magnets by correcting induced orbit shift”, *Phys. Rev. Accel. Beams*, vol. 25, no. 5, p. 052802, May 2022. doi:10.1103/PhysRevAccelBeams.25.052802
- [18] Xiaobiao Huang, “Beam-based Alignment (BBA) Simulations for the FCC-ee Lattice”, presented at the FCC-IS WP2 workshop, Angelicum, Rome, 2023, unpublished. <https://indico.cern.ch/event/1326738>
- [19] A G Mathewson and S Zhang, “Beam-gas ionisation cross sections at 7.0 TeV”, CERN, Geneva, Rep. LHC-VAC/AGM; Vacuum-Technical-Note-96-01, 1996. <https://cds.cern.ch/record/1489148>
- [20] Virgil L. Highland, “Some practical remarks on multiple scattering”, *Nuclear Instruments and Methods*, vol. 129, no. 2, pp. 497–499, 1975. doi:10.1016/0029-554X(75)90743-0
- [21] A. W. Chao and G. V. Stupakov, “Effect of feedback and noise on fast ion instability”, Rep. SLAC-PUB-7607, July 1997.
- [22] T. O. Raubenheimer and F. Zimmermann, “A Fast beam - ion instability in linear accelerators and storage rings”, *Phys. Rev. E*, vol. 52, pp. 5487–5497, 1995. doi:10.1103/PhysRevE.52.5487
- [23] Zhe Duan *et al.*, “Longitudinally Polarized Colliding Beams at the CEPC”, in *Proc. eeFACT’22*, 2023, pp. 97–102. doi:10.18429/JACoW-EEFACT2022-TUZAS0101
- [24] Tao Chen, Zhe Duan, Daheng Ji, and Dou Wang, “Booster free from spin resonance for future 100-km-scale circular e⁺e⁻ colliders”, *Phys. Rev. Accel. Beams*, vol. 26, no. 5, p. 051003, May 2023. doi:10.1103/PhysRevAccelBeams.26.051003
- [25] E. Gianfelice-Wendt, “Investigation of beam self-polarization in the future e⁺e⁻ circular collider”, *Phys. Rev. Accel. Beams*, vol. 19, no. 10, p. 101005, Oct. 2016. doi:10.1103/PhysRevAccelBeams.19.101005